

# State Discrimination Signal Nulling Receivers

F. E. Becerra,<sup>1</sup> J. Fan,<sup>1</sup> G. Baumgartner,<sup>2</sup> S. Polyakov,<sup>1</sup> J. Goldhar,<sup>3</sup> J. T. Kosloski,<sup>4</sup> and A. Migdall<sup>1</sup>

*1 Joint Quantum Institute, Department of Physics, University of Maryland,  
and National Institute of Standards and Technology,  
100 Bureau Drive, Gaithersburg, MD 20899, U. S. A.*

*2 Laboratory for Telecommunications Sciences, 8080 Greenmead Drive, College Park, MD 20740*

*3 Department of Electrical and Computer Engineering,  
2410 A.V. Williams Bldg., University of Maryland, College Park, MD 20742*

*4 Department of Electrical and Computer Engineering, Johns Hopkins University, Baltimore MD 21218  
Migdall@nist.gov*

## ABSTRACT

Optimized state-discrimination receiver strategies for nonorthogonal states can improve the capacity of the communication channels operating with error rates below the ones corresponding to conventional receivers. Coherent signal-nulling receivers use a local oscillator to null the signal state and perform the discrimination of the signal from an alphabet of nonorthogonal states. We describe our study of signal nulling for signals encoded in nonorthogonal phase states. The signal nulling discrimination setup is the first step for the experimental investigation of different discrimination strategies for receivers of coherent multi-phase encoded signals.

**Keywords:** State Discrimination, Classical Optical Communications, Interference, Optical receivers

## 1. INTRODUCTION

Quantum key distribution (QKD) allows for the generation of a secret key between a transmitter and a receiver for secure communications. It uses nonorthogonal states so that an eavesdropper cannot discriminate between these states with total certainty, and as a result the eavesdropping cannot be done without leaving a trace of its presence. When the nonorthogonal states used are coherent states, the inability of perfect state discrimination in the receiver limits the transmission bit rate, and in the case of classical communications imperfect state discrimination produces unavoidable errors in the decoded information [1, 2].

This has motivated the search for possible receivers and eavesdropper state discrimination strategies that minimize the probability of error below what is achievable with conventional receivers [3-7], or alternatively, to perform unambiguous state discrimination (USD) [8] with a nonzero probability of conclusive results. Additionally, different strategies have been found for receivers discriminating multiple nonorthogonal states [9, 10] surpassing the shot noise limit.

Signal-nulling receivers use a strong local oscillator (LO) and interferometric measurements to learn about the state of the signal through displacement operations [5]. Minimum-error-discrimination nulling receivers can achieve error probabilities below the conventional homodyne limit [2], and approach the quantum limits by using adaptive measurements, such as in the case of general conditional signal nulling [4, 6] which can reach the quantum limit (Helstrom bound) through application of a varying-intensity LO, or being suboptimal with a constant-intensity LO [11, 12]. Moreover, conditional and nonconditional signal-nulling receivers are suitable for error-free USD in the case of perfect signal nulling [13, 14] with a constant-intensity LO.

The efficiency of signal nulling and detection efficiency limits the error probability in the case of minimum-error discrimination and produces errors in the case of USD receivers. We describe here, our scheme for emulating discrimination receivers using perfect signal nulling, where the signal alphabet is composed by multiple coherent symmetric phase states [15]. The emulator design uses orthogonal polarizations for the signal and a strong LO at the entrance of the receiver, and performs signal nulling in different stages by polarization projection. We focus on the nulling of the input signal with a specific phase against the strong local oscillator, the projected total field, and the system losses. This emulator can in principle test different conditional and nonconditional signal-nulling receivers performing minimum-error discrimination and USD although we leave specific applications for future work.

## 2. SIGNAL-NULLING RECEIVERS USING A STRONG LOCAL OSCILLATOR

Coherent signal-nulling receivers measure a weak signal in a coherent state, belonging to an alphabet of nonorthogonal states, by mixing it with a strong LO and detecting the interference with a single photon detector. Signal nulling is defined as the total destructive interference achieved when a small fraction of the strong LO is combined with the signal in the case where the relative phase between signal and LO is  $\pi$ . A small signal to LO power ratio is implemented so that the most of the signal energy is used in the detection process. The receiver acquires information about the state of the signal from the detection result in a discrimination stage setup together with the LO setting (hypothesis phase) for that stage, and bases its decision on those two pieces of information depending on the particular strategy. Fig. 1 shows two possible state discrimination stages for signal nulling: (a) state discrimination stage using an unbalance beam splitter-combiner (uBS) to combine a small fraction of the LO with a large fraction of the signal arriving from separate optical paths. (b) The same process is achieved with a polarizer (or a polarization-based interferometer) when the signal and LO co-propagate with orthogonal polarizations and they mix in the polarizer oriented to project a small (large) fraction of the LO (signal) onto the signal polarization. A single photon detector (SPD) measures the interference in the total field and the result is used according to the specific strategy.

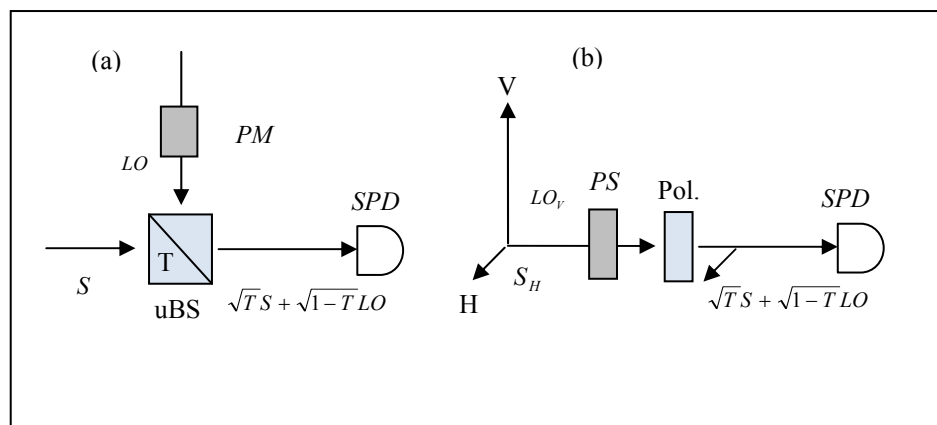


Figure 1. State Discrimination stages detecting the interference of the signal ( $S$ ) and LO (a) arriving from different optical paths with equal polarizations using a high transmittance ( $T$ ) beam splitter (uBS) for the signal (b) copropagating with orthogonal polarization modes using a polarizer oriented to transmit and mix a large fraction of the signal with a small fraction of the LO where the transmittance for the signal is  $T=\cos(\theta)$  (where the polarizer angle from the horizontal is  $\theta=0$ ). Single-photon detectors measure the interference after projection of the fields. The LO hypothesis is prepared before interfering with the signal according to the specific strategy. Phase modulators (PM) for (a) or phase shifters (PS) for (b) prepare the hypothesis phase of the LO to test phase encoded signals.

In general for multi-element signal alphabets greater than 2, tests of different signal hypotheses are required. To implement this, the receiver can distribute the energy of the signal and the LO among several discrimination stages (or time bins in the case of feedback receivers). In each stage (time bin), the LO parameters are set, or adapted, to null the desired signal depending on the modulation parameter (i. e., intensity modulation, phase modulation, etc.) and the particular strategy.

For conditional signal-nulling receivers, the information gained in a particular discrimination stage setup (or time bin) is used to adapt a posterior measurement in a subsequent discrimination stage setup (or time bin) to best measure the signal, i.e. make the measurement that would provide maximum information [4, 6, 9, 10, 13, 15]. Conditional receivers with multiple discrimination stages are feed-forward receivers, and conditional receivers using time bins for adaptive measurements are feedback receivers. In this discussion of feedback and feed forward schemes, we note that while feedback receivers limit the transmission rate due to finite feedback bandwidths, feed-forward receivers allow scalability to high transmission rates.

Nonconditional-nulling receivers can use a single- or a multiple-number of stages. Their practical implementation is easier and can still surpass the classical HL or shot noise limit of conventional minimum-error-discrimination receivers [5, 7], and these receivers can also perform USD [13, 14]. However, their performance is suboptimal in comparison to conditional receivers.

Figure 2 shows an example of a receiver with multiple stages where the signal and LO are in orthogonal polarizations. In this case the signal combines with a strong LO with orthogonal polarization at the entrance of the receiver using a polarizing beam splitter (PBS). The received signal can be, for instance, a weak coherent state in a phase modulation format corresponding to quadrature phase shift keying (QPSK), where the possible phases of the signal are:  $\{0, \pi/2, \pi, 3\pi/2\}$  as shown in the inset of Fig. 2. The copropagating signal and LO are distributed to different polarization-based state discrimination stages as shown in Figure 1 (b). While nonconditional-nulling receivers have fixed LO settings in each discrimination stage, conditional receivers adapt the LO settings in subsequent stages with a policy specified by the particular discrimination strategy.

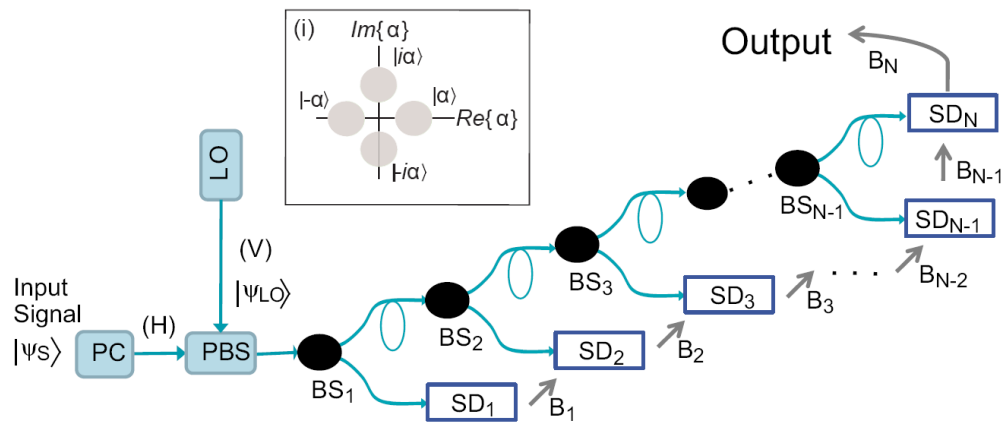


Figure 2. State-discrimination receiver. The signal and a strong LO with orthogonal polarizations are combined in a single beam with a polarizing beam splitter (PBS). The copropagating signal and LO with an intensity signal/LO ratio of  $\approx 1/100$  enter an array of beam splitters (BS) that distribute the energy of the beam in the polarization-based-discrimination stages shown in Figure 1 (b). Discrimination stages prepare the LO phase using phase shifters (PS) and perform signal nulling using polarizers.

### 3. POLARIZATION-BASED SIGNAL-NULLING STAGES

The state-discrimination receiver of Figure 2 can be implemented using fiber-coupled components or free-space links. We investigate the performance of the polarization-based signal-nulling stages for free-space links where no polarization-dispersion compensation is required. We use off-the-shelf components to test the feasibility for applications of real receiver structures.

We assume that the signal is in a coherent state with amplitude  $\alpha_s$  and phase  $\phi$  with horizontal polarization (H), and the strong LO has amplitude  $\alpha_{LO}$  with horizontal vertical (V). The signal and LO are combined with the PBS creating the state of the field:

$$|\Psi(\phi)\rangle = \begin{bmatrix} e^{i\phi} \alpha_s \\ -\alpha_{LO} \end{bmatrix} \quad (1)$$

where  $|a\rangle_H = \begin{pmatrix} a \\ 0 \end{pmatrix}$  and  $|b\rangle_V = \begin{pmatrix} 0 \\ b \end{pmatrix}$  are the vector representation of the polarizations. The field described in Eq.

(1) is in general distributed among  $N$  discrimination stages. In a particular discrimination stage, the LO is prepared with a phase  $\delta$  to test the phase state of the signal. This phase is prepared by a phase shifter (PS) that sets the relative phase between the signal and LO to  $\phi - \delta + \pi$ :

$$|\Psi(\phi)\rangle = \frac{1}{\sqrt{N}} \begin{bmatrix} e^{i\phi} \alpha_S \\ -e^{i\delta} \alpha_{LO} \end{bmatrix}. \quad (2)$$

The polarizer in the stage is oriented so that the transmission of the H polarization is  $T$ , and it transfers a fraction  $1-T$  of the LO. The field after the projection is:

$$\langle \bar{p} | \Psi(\phi, \delta) \rangle = \frac{1}{\sqrt{N}} \left( \sqrt{T} \sqrt{n_S} e^{i\phi} - \sqrt{1-T} \sqrt{n_{LO}} e^{i\delta} \right), \quad (3)$$

where  $\bar{p} = \begin{pmatrix} \sqrt{T} \\ \sqrt{1-T} \end{pmatrix}$  is the projection due to the polarizer and  $n_i = |\alpha_i|^2$  is the average photon number of the field. The mean photon number of the total field at the detector is:

$$\langle n(\phi, \delta) \rangle = \frac{1}{N} \left( n_S T + n_{LO} (1-T) - 2 \sqrt{n_S n_{LO} (1-T) T} \cos(\phi - \delta) \right). \quad (4)$$

To produce a null detection event,  $\delta = \phi$ , the signal and LO strengths have to be the same. This is satisfied when

$$T = \frac{n_{LO}}{n_S + n_{LO}};$$

$$\langle n(\phi, \delta) \rangle = n_S \frac{T}{N} |e^{i\phi} - e^{i\delta}|^2. \quad (5)$$

Note that the condition  $T \approx 1$  follows from  $n_{LO} \gg n_S$  for average photon numbers of the LO and signal at the entrance of the receiver. Based on the hypothesis and the result of the detection event for a given photon number, the nulling receiver learns about the possible state of the signal (for example by calculating a posteriori probabilities for the possible input states and using Bayes rule) and can use this information for state discrimination with any specific strategy.

We experimentally study the performance of a nulling-state-discrimination stage for nonorthogonal-phase-coherent states in a QPSK format for the case when the signal and LO have orthogonal polarizations as described in Fig. 1 (b). We use a birefringent quartz plate, with its optical axis aligned horizontally, as a phase shifter (PS in Fig. 1 (b)) between the signal (H polarization) and LO (V polarization). The polarizer consists of a PBS together with a half-wave plate (HWP), and we analyze the performance of the discrimination stage by detecting the interference using a photodiode. Single-photon counting is only required for the study of the statistical Poissonian probabilities as a function of mean photon number to test specific state discrimination strategies. We prepare the signal and LO state from a single beam of a laser at 633 nm with an intensity variation smaller than 0.1% and polarized in the vertical direction (LO polarization) with an extinction ratio greater than  $10^5$ . We use a HWP and a quarter wave plate to prepare the four phase states of the signal with respect to the LO:  $\{0, \pi/2, \pi, 3\pi/2\}$ , with a signal-to-LO intensity ratio of 1/100.

The relative phase shift induced by the PS is proportional to the length of the propagation path of the light through the quartz. We use a tilt (rotation around the vertical axis of the plate and perpendicular to the propagation direction)

to increase the effective optical path and produce a continuous relative phase shift between the signal and LO fields. In this way we can project the signal and LO with any relative phase for a given input state. The matrix representation of a phase shifter between V and H (in this case the quartz plate) is:

$$QP(\theta_0, \delta) = \begin{bmatrix} \cos^2 \theta_0 + e^{i\delta} \sin^2 \theta_0 & (1 - e^{i\delta}) \cos \theta_0 \sin \theta_0 \\ (1 - e^{i\delta}) \cos \theta_0 \sin \theta_0 & \sin^2 \theta_0 + e^{i\delta} \cos^2 \theta_0 \end{bmatrix}, \quad (6)$$

where  $\delta$  is the induced phase shift between H and V polarizations and  $\theta_0$  is the rotation angle of the PS with respect to H. When the optical axis of the quartz plate is aligned with the horizontal,  $\theta_0 = 0$ , the quartz plate changes the relative phase without mixing the polarizations:

$$QP(\theta_0, \delta) = \begin{bmatrix} 1 & 0 \\ 0 & e^{i\delta} \end{bmatrix}. \quad (7)$$

The induced phase  $\delta$  depends on the properties of the material, the propagation distance of the light inside the medium and on the wavelength [16]:

$$\delta = \frac{2\pi L \Delta n}{\lambda}, \quad (8)$$

where  $\Delta n = |n_e - n_o| = 0.0091$  is the difference of refractive index of the ordinary ( $n_o$ ) and extraordinary ( $n_e$ ) rays in quartz [17],  $\lambda = 633$  nm for our experiment and  $L$  is the propagation distance of the light in the medium. For a quartz plate of thickness  $d \approx 1$  mm, the propagation distance as a function of tilt angle  $\theta$  (rotation around the vertical axis perpendicular to the beam propagation direction) is:

$$L = d \left[ \cos \left\{ \arcsin \left( \frac{n_{\text{air}}}{n_1} \sin \theta \right) \right\} \right]^{-1}, \quad (9)$$

where  $n_{\text{air}} \approx 1$  and  $n_1 \approx 1.545$  are the indexes of refraction of air and quartz, respectively. Eq. (4) together with Eq. (8) describe the mean photon number in the detector as a function of LO phase  $\delta$  for a given signal input state  $\phi$ . We test the signal-nulling discrimination stage using a continuous wave beam as a function of phase shift for different input signal phase states for a signal/ LO intensity ratio of 1/100.

Figure 3 shows the experimental observations for signal nulling as a function of tilt angle of the QP for four signal phase states  $\phi = \{0, \pi/2, \pi, 3\pi/2\}$  corresponding to QPSK modulation format. We observe that for every input signal phase, there is a tilt angle  $\beta$  (nulling angle) corresponding to destructive interference, i.e. signal nulling. We compare these measurements with the theoretical projected intensities for the experimental parameters using the average photon number in Eq. (4) and the phase shift induced by the QP from Eqs. (8) and (9).

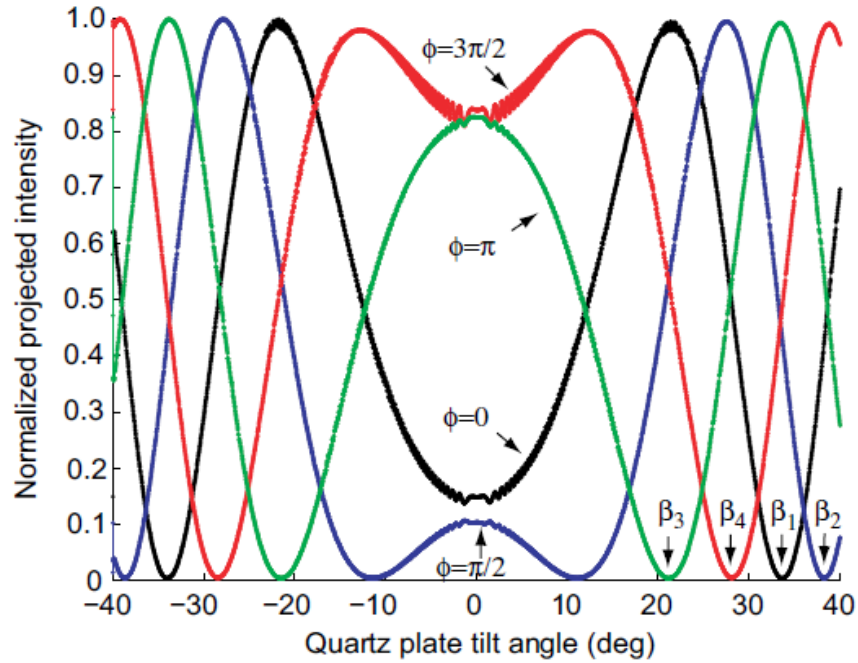


Figure 3. Projected and normalized intensity of the total field containing the signal and LO after the polarizer for input signals in a QPSK format as a function of the QP tilt angle working as a continuous phase shifter.

Figure 4 shows the fits to the experimental curves from Fig. 3 where we use the input state phase, the amplitude, and the background as free parameters. We observe an excellent agreement between the theoretical predictions and the experimental observations for the projected intensities of the total field.

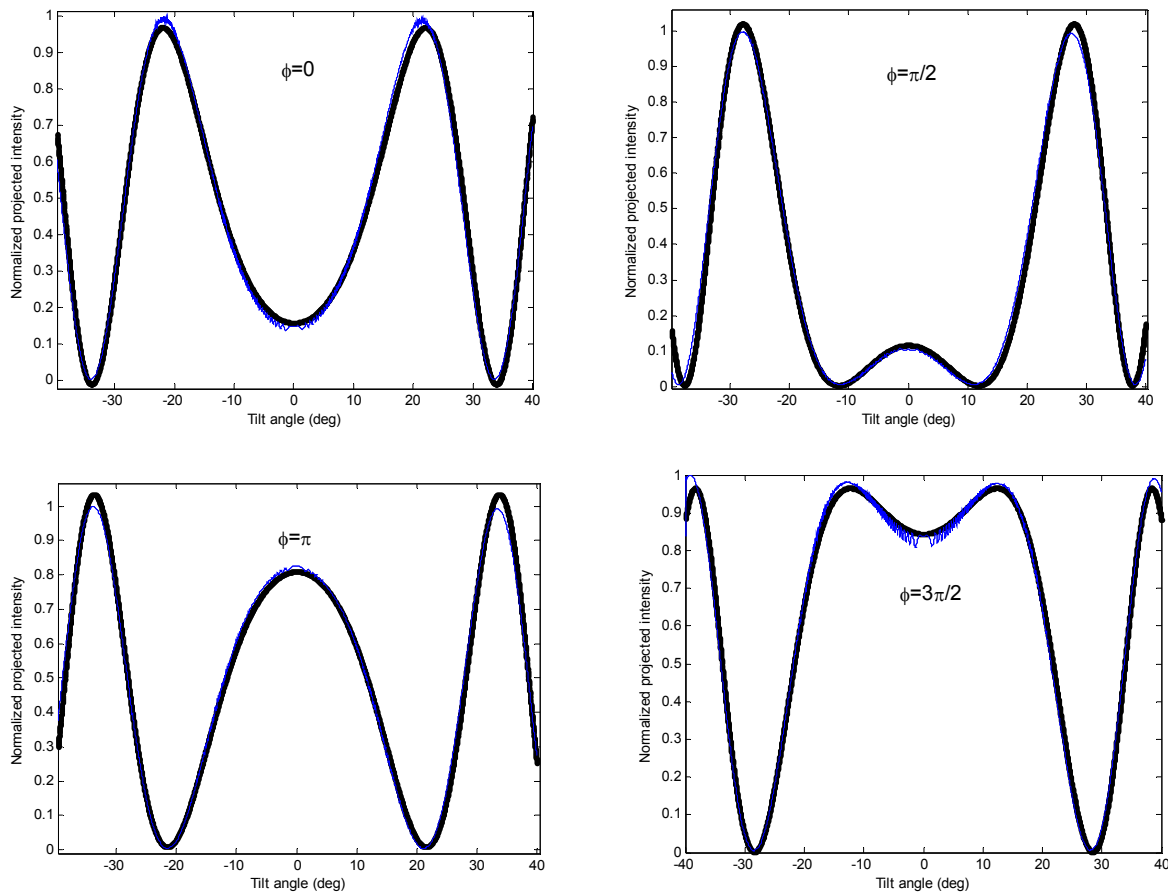


Figure 4. Experimental (thin blue lines) and theoretical (thick black lines) projected intensity of the total field as a function of the QP tilt angle for input phase states  $\phi = \{0, \pi/2, \pi, 3\pi/2\}$ .

We use these fits to obtain the nulling angles and the expected phase shift of the QP for a general input state, and calibration of the QP alignment. The advantage of this setup is that it can be easily generalized to higher modulation formats, and can test real implementations of different state discrimination strategies with a single- or multiple-discrimination stages.

The efficiency of signal nulling is related with the fringe visibility. This is an important parameter in the performance of any nulling receivers, since it indicates how well we can identify the signal with the application of the LO with the appropriate phase. The fringe visibility extracted from the fit for the particular discrimination stage described in Fig. 4 is  $V_{\text{Fit}}=98.5(5)\%$  that is consistent with our measurement of  $V_{\text{Exp}}=99.0(5)\%$ , where the uncertainties are 1- $\sigma$  standard deviations.

## 4. CONCLUSIONS

We investigated the signal-nulling process for coherent-signal-nulling receivers for the discrimination of nonorthogonal signal phase states. We analyzed the case for symmetric phase coherent states for application to a quadrature-phase-shift keying communication scheme where the local oscillator reference is orthogonally polarized with respect to the signal. We used a birefringent plate to prepare the reference field for signal nulling of a particular signal state. We observed signal nulling for QPSK signals with high visibility. This experimental setup can test

different state-discrimination strategies when used with single-photon counting and postprocessing of the collected data. In addition, it can be generalized to test discrimination strategies for coherent signals in higher phase modulation formats and to verify the operation and practicality of those schemes. Such test results provide a clear path toward nonorthogonal unambiguous multi-state discrimination or nonorthogonal multi-state discrimination with error rates below the standard quantum limits.

## REFERENCES

- [1] B. Huttner, N. Imoto, N. Gisin, and T. Mor, *Phys. Rev. A* **51**, 1863 (1995).
- [2] J. G. Proakis, [Digital Communications], 4th Ed., McGraw-Hill, New York, (2000).
- [3] C. W. Helstrom, [Quantum detection and estimation theory], Mathematics in Science and Engineering Vol. 123, Academic Press, New York, (1976).
- [4] S. J. Dolinar, "A optimum receiver for the binary coherent state quantum channel", MIT Quarterly Progress Report No. 111, unpublished (1973).
- [5] R. S. Kennedy, "A near-optimum receiver for the binary coherent state quantum channel", MIT Technical Report No. 110, unpublished (1972).
- [6] M. Takeoka, M. Sasaki, P. van Loock, and N. Lutkenhaus, *Phys. Rev. A* **71**, 022318 (2005).
- [7] C. Wittmann, M. Takeoka, K. N. Cassemiro, M. Sasaki, G. Leuchs, and U. L. Andersen, *Phys. Rev. Lett.* **101**, 210501 (2008).
- [8] I. D. Ivanovic, *Phys. Lett. A* **123**, 257 (1987), D. Dieks, *Phys. Lett. A* **126**, 303 (1988), A. Peres, *Phys. Lett. A* **128**, 19 (1988).
- [9] R. S. Bondurant, *Opt. Lett.* **18**, 1896 (1993).
- [10] M. Usuga, C. Muller, C. Wittmann, M. Takeoka, U. Andersen, and G. Leuchs, in *Lasers and Electro-Optics 2009 and the European Quantum Electronics Conference. CLEO Europe - EQEC 2009*, p. 1 (2009).
- [11] S. Guha, J. L. Habif and M. Takeoka, *Journal of Modern Optics*, **58**, 257 (2011).
- [12] Dolinar S. J., TDA Progress Report, 42-72 October 1982, NASA: Pasadena, CA (1983).
- [13] S. J. van Enk, *Phys. Rev. A* **66**, 042313 (2002).
- [14] M. Sedlák, M. Zíman, O. Příbyla, V. Bužek, and M. Hillery, *Phys. Rev. A* **76**, 022326 (2007).
- [15] F. E. Becerra, J. Fan, G. Baumgartner, S. Polyakov, J. Goldhar, J. T. Kosloski, and A. Migdall, in process.
- [16] B. E. A. Saleh and M. C. Tehch, [Fundamentals of Photonics], Wiley Series in Pure and Applied Optics, New Jersey, (2007).
- [17] E. D. Palik, [Handbook of Optical Constants of Solids], Academic Press, San Diego CA, (1989).